A new criterion to assess distributional homogeneity in hyperspectral images of solid pharmaceutical dosage forms.

Pierre-Yves Sacré[a,*], Pierre Lebrun[b], Pierre-François Chavez[a], Charlotte De Bleye[a], Lauranne Netchacovitch[a], Eric Rozet[a], Régis Klinkenberg[c], Bruno Streel[c], Philippe Hubert[a], Eric Ziemons[a]

[a] University of Liege (ULg), Department of Pharmacy, CIRM, Laboratory of Analytical Chemistry, CHU, B36, 4000 Liege, Belgium

[b] Arlenda S.A., Avenue de l'Hopital, 1, B-4000 Liege, Belgium

[c] Galéphar Research Center M/F, rue du Parc Industriel 39, 6900 Marche en Famenne, Belgium

Abstract

During galenic formulation development, homogeneity of distribution is a critical parameter to check since it may influence activity and safety of the drug. Raman hyperspectral imaging is a technique of choice for assessing the distributional homogeneity of compounds of interest. Indeed, the combination of both spectroscopic and spatial information provides a detailed knowledge of chemical composition and component distribution.

Actually, most authors assess homogeneity using parameters of the histogram of intensities (e.g. mean, skewness and kurtosis). However, this approach does not take into account spatial information and loses the main advantage of imaging. To overcome this limitation, we propose a new criterion: Distributional Homogeneity Index (DHI). DHI has been tested on simulated maps and formulation development samples. The distribution maps of the samples were obtained without validated calibration model since different formulations were under investigation. The results obtained showed a linear relationship between content uniformity values and DHI values of distribution maps. Therefore, DHI methodology appears to be a

suitable tool for the analysis of homogeneity of distribution maps even without calibration during formulation development.

Keywords:

Hyperspectral imaging; Raman spectroscopy; distributional homogeneity; macropixels; pharmaceutical formulation.

*Corresponding Author. Tel.: +32 4 366 4324; Fax: +32 4 366 4317

E-mail address: pysacre@ulg.ac.be

Address: Laboratory of Analytical Chemistry, CIRM, Department of Pharmacy, University of Liege, 1 Avenue de l'Hopital, B36, B-4000 Liege, Belgium

1. Introduction

During pharmaceutical development, assessment of the homogeneity of powder blends is a critical step that will impact both medicine safety and efficacy. Actually, HPLC is the commonly used technique consuming time and requiring a lot of resources. This is the reason why NIR and Raman spectroscopies have been more and more used to study powder blend processes [1-3]. However, none of these techniques can determine the spatial distribution of the components in the final product.

Hyperspectral imaging combines spectral and spatial information. Therefore, it has gained in importance in pharmaceutical analysis during the last decade. Indeed, it allows obtaining simultaneously the API (Active Pharmaceutical Ingredient) concentration and its corresponding distribution map [4].

In the pharmaceutical field, hyperspectral techniques are mainly based on Raman, near-infrared (NIR-CI) or mid-infrared (MIR-CI) spectroscopies and have been used to obtain quantitative distribution maps of pharmaceutical ingredients [5-7], to detect and quantify polymorphs [8, 9], to characterize particle size [10], to detect counterfeit medicines [11] and to characterize blending conditions [12, 13].

Several approaches have been used to assess the distributional homogeneity in an objective way. Most of them used a quantitative model to obtain distribution maps and then analyzed the histogram of pixel concentrations [14-17]. Histograms parameters (mean, standard deviation, skewness and kurtosis) are useful to assess the “constitutional homogeneity” which is the dispersion of pixel concentration values [6]. However, two maps may have exactly the

same constitutional homogeneity while being spatially totally different. This is why it is also important to assess the distributional homogeneity.

Usually, distributional homogeneity is assessed by visual inspection of distribution maps. This approach clearly lacks objectivity and if the difference between the two maps is tight, it is impossible to unequivocally declare which one is the most homogeneous.

Therefore, Rosas et al. [18-20] developed a criterion to obtain an objective value of distributional homogeneity. This criterion is based on the analysis of the Poole index of non-overlapping macropixels. However, this approach has several limitations. As it works with non-overlapping macropixels, it is quickly limited for the analysis of small distribution maps. Furthermore, studied map must be binarized. This binarization step is inevitably a source of error. Therefore, it appears that it could be advantageous to develop a new criterion which could analyze small maps and which would need as few input and pre-processing as possible to avoid as much error as possible.

In this paper, we describe a new criterion called Distributional Homogeneity Index (DHI). This index can be performed on small maps with continuous values. Relevance of the developed DHI has been tested on simulated distribution maps of controlled increasing homogeneity.

Secondly, DHI has been applied on several developed formulations with different content uniformity values. As these formulations were under investigation, no quantitative model (e.g. partial least square model) should be built. DHI was then tested on distribution maps obtained by semi-quantitative methods.

2. Material and methods

2.1. Samples

Several pilot blends of 8 kg were produced with different blending conditions, API particle size and excipients grade. Final concentration of API was of 8.4 % (w/w). These blends were then pressed in tablets of 80 mg and of 5 mm of diameter.

Tablets were collected in a stratified way (begin, middle and end of the tableting) for several blends. For each blend, begin, middle and end samples were considered as different batches. Batch selection for hyperspectral analysis was performed choosing a specific blend and a specific tableting time. To do so, ten tablets per batch were randomly chosen, assayed by HPLC and the content uniformity (expressed as relative standard deviation, RSD %) and the European Pharmacopoeia's acceptance value [21] were calculated.

Batches with different content uniformity and acceptance values ranging from 0.46 % to 11.04 % and from 1.10 to 29.41 respectively were selected. Once the batch selected, ten other tablets were randomly chosen and analyzed by hyperspectral Raman imaging.

For confidentiality reasons, neither HPLC method nor information of tablet's qualitative composition and blending conditions can be presented. Tablet's quantitative composition is presented in supplementary Table S1. Spectral similarities between tablet's components are presented as correlation coefficient values in supplementary Table S2.

2.2. Instrumentation

Raman hyperspectral images were collected with a dispersive Raman spectrometer RamanStation 400F (Perkin Elmer, MA, USA) equipped with a two-dimensional CCD detector (1024 × 256 pixel sensor). The laser excitation wavelength used was 785 nm with a power of 100 mW.

The measured spectral region was 1622-90 cm^{-1} and the spectral resolution was equal to 2 cm^{-1}. One accumulation with a 1 second exposure time was performed per sample mapping point. The distance between 2 consecutives mapping measurements was fixed at 100 µm. Background acquisition during mapping was repeated each 20 minutes. The spectra were collected with the Spectrum 6.3.2.0151 (Perkin Elmer) software.

The analyzed tablet surface was prepared beforehand with a Leica EM Rapid milling system equipped with a tungsten carbide miller (Leica Microsystems GmbH, Wetzlar, Germany).

Tablets were circular with a diameter of 6 mm (area of 28 mm^2). Measured maps represented the greatest square possible with a map size of 40x40 and a step size of 100 µm. A total surface of 16 mm^2 was covered.

Ten tablets per batch were analyzed.

2.3. Data processing

Once acquired, the hyperspectral images underwent preprocessing and multivariate analysis to extract useful information.

First, hyperspectral data cubes ($M \times N \times \lambda$) were unfolded into a two-dimensional array ($MN \times \lambda$) where M and N are the spatial information and λ the spectral information. Once unfolded, Raman spectra were baseline corrected using the Asymmetric Least Squares (AsLS) algorithm [22] with a λ value of 10^5 and a p value of 0.001.

Then, cosmic rays have been removed using the algorithm developed by Sabin et al. [23] with a parameter k set at 15.

Two multivariate data analysis approaches were used:

Classical Least Squares (CLS) regression: Distribution maps were obtained using CLS regression. This method assumes that Beer–Lambert's law is respected and that the sum of the individual absorbance for each component equals the total absorbance for each pixel. Therefore, it computes the concentration of each component by direct regression of the hyperspectral data cube by using the pure spectra.

It is a very easy and fast method but it is not flexible at all and any variability not reflected in the pure spectrum may affect the results [24]. Therefore, to obtain pure spectra as representative as possible, they have been resolved with Multivariate Curve Resolution – Alternating Least Squares (MCR-ALS).

All analyzed maps were assembled and one every tenth spectrum was retained. Then, resolution of the pure spectra of each component was performed by the MCR-ALS toolbox [25-27]. Initial spectra estimates were obtained by simple-to-use-interactive self-modelling mixture analysis (SIMPLISMA) [28]. The constraints applied in the resolution analysis were non-negativity in the concentration profiles and spectra.

The advantage of image multiset analysis by MCR-ALS is the higher robustness of the resolved spectra and concentration maps.

Refolded CLS scores of the API were then used as distribution map.

Principal Component Analysis (PCA): PCA is a variable reduction technique, which reduces the number of variables by making linear combinations of the original variables. These combinations are called the principal components (PC) and are defined in such way that they explain the highest (remaining) variability in the data and are by definition orthogonal.

The importance of the original variables in the definition of a principal component is represented by its loadings and the projections of the objects onto the principal components are called the scores of the objects [29].

Unfolded preprocessed data cubes were mean centered before PCA analysis. The first PC was linked to the API with a good confidence since the correlation coefficient between the first loading and the pure API spectrum is higher than 0.966 (see supplementary Table S3). However, such a strategy is only applicable if a sufficient proof of correlation between the loading and the studied compound is obtained. Refolded scores of the first PC were then used as distribution map of the API.

DHI and preprocessing of hyperspectral data cubes were performed using routines written in Matlab R2013a (The Mathworks, Natick, MA, USA). Multivariate data analysis was performed using the PLS_Toolbox 7.0.3 (Wenatchee, WA, USA) running on Matlab and MCR-ALS was performed using the toolbox described in [27].

Analysis of experimental data was performed on Microsoft Excel 2010 (Microsoft, Albuquerque, NM, USA).

3. Results and discussion

3.1. Distributional Homogeneity Index (DHI)

As stated before, conventional homogeneity testing of distribution maps consists of analyzing the histogram of pixel intensities. However, this technique is highly dependent on the spatial resolution of the hyperspectral imaging technique. Furthermore, this approach cannot differentiate two distribution maps with different spatial distribution if they have the same pixel intensities.

Therefore, a subsampling technique is necessary to evaluate the spatial homogeneity of a distribution map. This technique called macropixel analysis was first introduced by Hamad et al. [30]. A macropixel is a "square cluster of neighboring pixels with an intensity value equal to the average value of the included pixels". Macropixel size can vary from a single pixel size to the entire distribution map size.

The distribution map is first sampled by all possible macropixel of size 2x2 original pixel size. Then, all macropixels of size 3x3 are evaluated. The computation goes on with unit macropixel size increase until macropixel size equals the whole distribution map size. This approach is called the Continuous-Level Moving Block (CLMB) [30]. Therefore, for a defined macropixel size, there exists a total number of macropixels of (image size – macropixel size +1)^2.

For each macropixel size, the standard deviation of the macropixel value is computed. Then, standard deviation is plotted against the macropixel size to obtain the so-called "homogeneity curve" [31].

Once the homogeneity curve obtained for the studied distribution map, the map is randomized and the homogeneity curve of the random map is computed. DHI value is obtained by the ratio of the area under the homogeneity curve (AUC) of the studied map and the area under the homogeneity curve of the randomized map (Figure 1).

Because of the randomization step, many simulations are necessary (generally 50 to 100 simulations) to compute a mean DHI value assorted with a standard deviation value.

It is now obvious that DHI is rather an inhomogeneity index than a homogeneity index as its value increases as the homogeneity of the distribution map decreases.

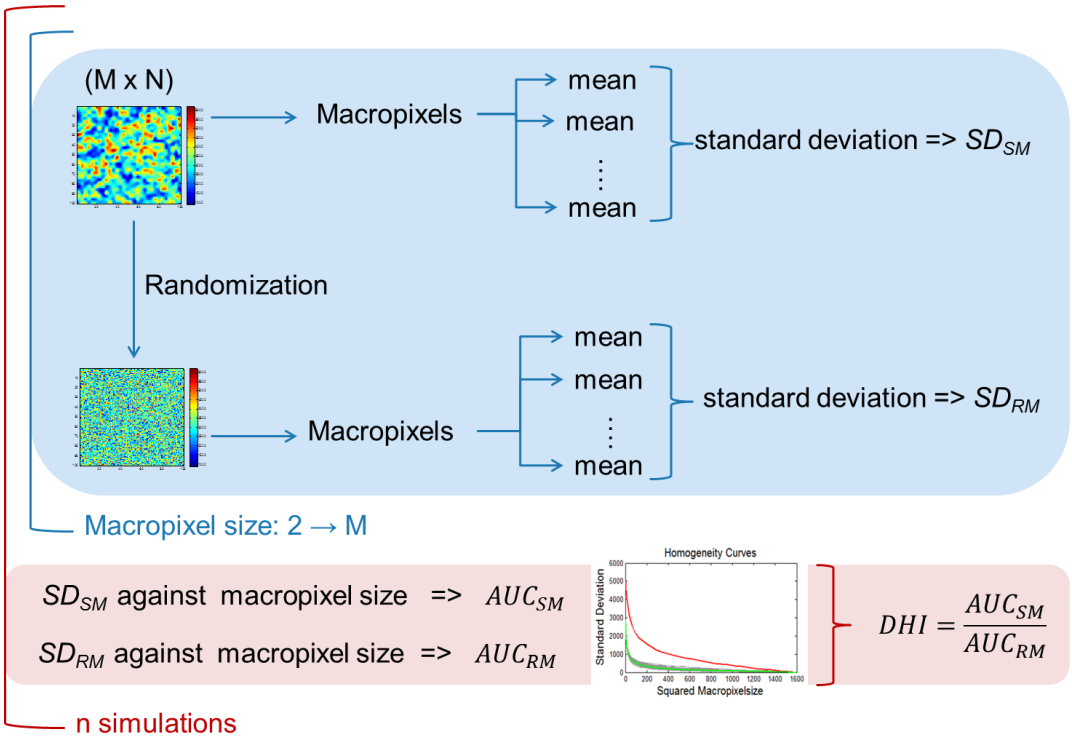

Figure 1: Methodology to compute the Distributional Homogeneity Index (DHI).

3.2. Test of DHI with controlled homogeneity maps

In order to test the properties of DHI and to evaluate the relationship between DHI and distribution map homogeneity, controlled homogeneity maps were constructed. These maps were composed of 50 % pseudorandom values from the standard uniform distribution on the open interval (0, 1). The other half is composed of zeros.

Therefore, a map of 10 % of controlled homogeneity means that a half of the image is composed of a random mix of 95 % of pseudorandom values and 5 % of zeros and the other half is composed of 95 % of zeros and 5 % of pseudorandom values. Doing so, one has an image with a total randomization of 10 % of the values keeping 90 % of the values divided in each half.

Indeed, a 100 % controlled homogeneity map means that each half has 50 % of zeros and 50 % of pseudorandom values randomly mixed.

Such simulated maps mimic well distribution maps and allow testing DHI on continuous values maps. Indeed, in the method developed by Rosas et al. [18-20], distribution maps are binarized prior to homogeneity evaluation. However, the threshold selection to achieve this binarization remains a non-trivial task and can therefore greatly affect the homogeneity measured. It appeared to us that the opportunity to work with continuous values maps could greatly ease the analysis.

Controlled homogeneity maps of different sizes were built with homogeneity ranging from 90 % to 10 %. Extreme homogeneity situations of 0 % and 100 % were avoided due to their unreal character that could mislead us in our conclusions. These maps were simulated four times and the DHI were computed.

As one can see on Figure 2b, a direct linear relationship is found between DHI values and controlled homogeneity with coefficient of determination (R^2) values higher than 0.99. Another important observation is that DHI values and best fit lines are different for each map size. Therefore, if one wants to compare two formulations, the analysis must be performed with the same parameters and the same map size.

DHI has also been tested on 60x60 simulated maps with an varying proportion of lines of zeros and of lines of random values: 10/50, 20/40, 30/30, 40/20 and 50/10, respectively. Figure 3b shows the corresponding DHI values plotted against controlled homogeneity. As expected, simulated maps with equal proportion of random values and zeros have the higher DHI denoting the lowest homogeneity. Simulated maps with a higher proportion of zeros have higher DHI considering their opposite with a higher proportion of random values. This can be explained by the fact that DHI is based on the ratio of the AUC of the studied map and the AUC of the randomized studied map. Therefore, simulated maps with a higher proportion

of random values are more similar to the randomized map than their opposite and appear slightly more homogeneous (smaller DHI).

This reinforces the fact that DHI must be performed only to check the homogeneity of a defined formulation. If one wants to compare many formulations with different API concentrations, preliminary tests are needed to confirm pertinence of future results.

a.

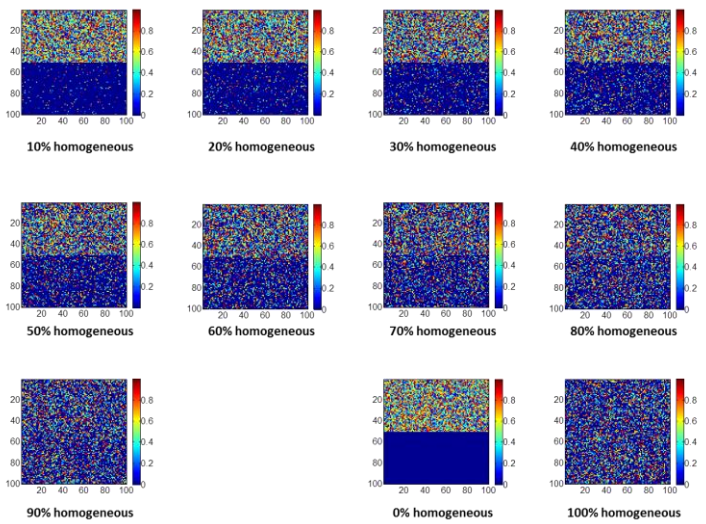

b.

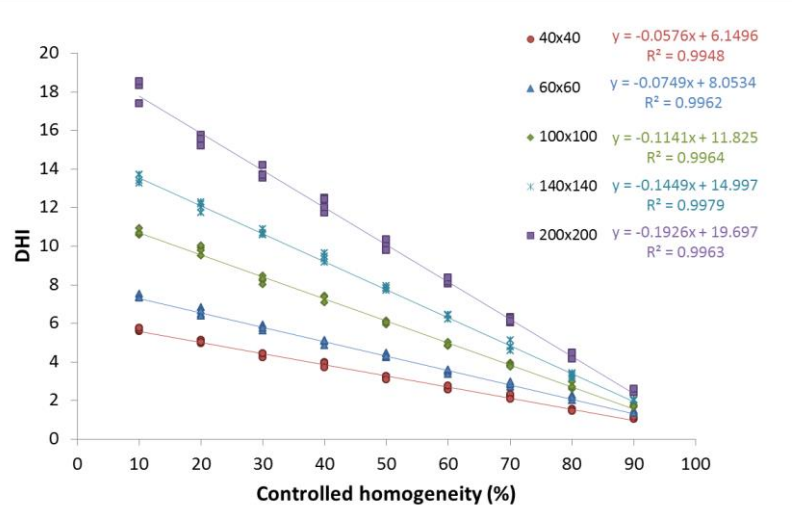

Figure 2: *a) Simulated distribution maps of size 100x100 with a proportion zeros and continuous values of 1:1. Extreme simulated maps (0 and 100 % of controlled homogeneity) are shown for illustration but were not analyzed by DHI.*

b) Plot showing the relationship between DHI values and the controlled homogeneity of the simulated distribution maps of size 40x40 (red circles), 60x60 (blue triangles), 100x100 (green diamond-shaped), 140x140 (turquoise crosses) and 160x160 (violet squares). Each controlled homogeneity map has been simulated four times. Best fit linear relationship was drawn with the four computed DHI values. Equation and coefficient of determination of corresponding best fit lines are shown.

a.

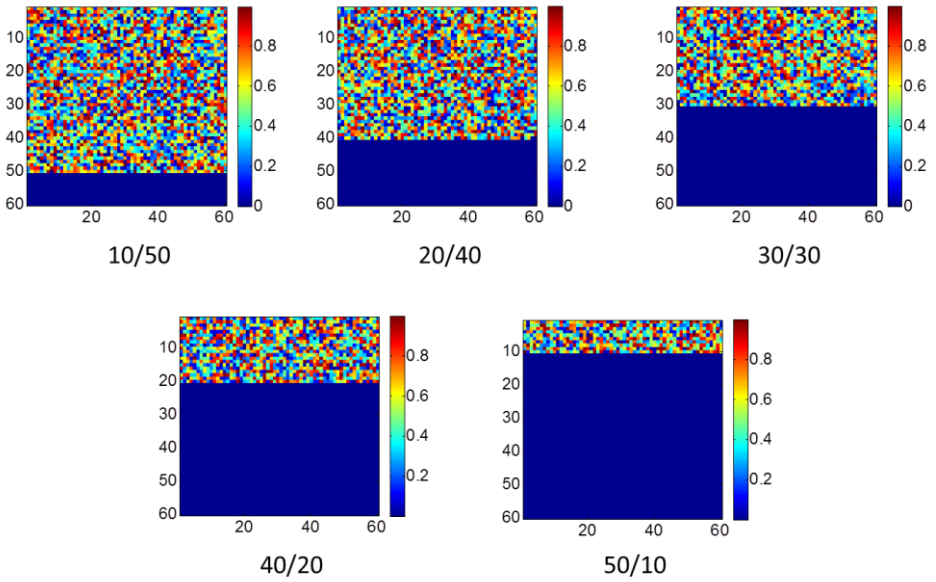

b.

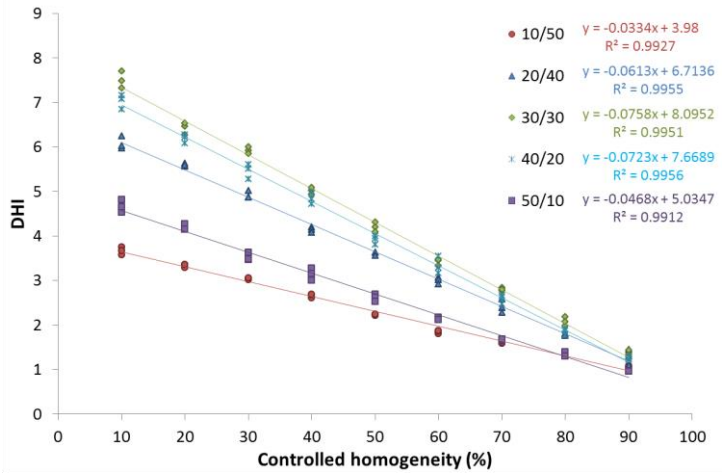

Figure 3: *a) Simulated distribution maps of size 60x60 with a growing proportion of zeros. For better visualization, only the maps of 0 % controlled homogeneity are shown.*

b) Plot showing the relationship between DHI values and the controlled homogeneity of the simulated distribution maps of size 60x60. Different proportions of zeros and continuous values of respectively 10/50 (red circles), 20/40 (blue triangles), 30/30 (green diamond-shaped), 40/20 (turquoise crosses) and 50/10 (violet squares) were analyzed. Each controlled homogeneity map has been simulated three times. Best fit linear relationship was drawn with the four computed DHI values. Equation and coefficient of determination of corresponding best fit lines are shown.

3.3. Analysis of real samples

As DHI represents spatial heterogeneity in API distribution, it has been decided to validate it with the well-known content uniformity test. The main idea was to develop a non-destructive and ecological friendly test that could be used by pharmaceutical industry while developing new formulations. Once prepared (milled), tablet are not destroyed by hyperspectral imaging and could therefore stay in a sample bank for further analysis or even inspections.

During formulation development, five batches of tablets were produced with content uniformity ranging from 0.46 % to 11.04 %. These batches represent well the variability that can be encountered during formulation development: different API particle size, excipient grades and blending conditions.

Once obtained, the hyperspectral images were processed and the distribution maps were obtained by CLS or PCA analysis (see section 2.3). DHI were computed on distribution maps obtained by the two methods.

Figure 4 shows the obtained content uniformity values plotted against the measured DHI values. As can be seen, a linear relationship (R^2 close to 0.99) is observed between DHI and content uniformity values validating the DHI methodology with real pharmaceutical samples. Another interesting observation is that DHI values measured from distribution maps obtained by both CLS and PCA are comparable (Table 1).

These observations constitute a major advantage of the DHI methodology since it is now possible to determine which formulation is the more homogeneous with neither any calibration dataset nor wet chemistry step. Indeed, multivariate calibration is difficult to implement since it necessitates the production of calibration samples with different nominal concentrations. Furthermore, any change in formulation leads to a complete re-development of the calibration model which is clearly not possible during formulation development step.

Hyperspectral imaging enables a fast analysis of different formulations while keeping prepared samples in a sample bank for any further analysis.

Table 1: Acceptance values, content uniformity and mean DHI values computed on distribution maps obtained by both CLS and PCA for the five developed formulations (batches A-E).

Batch Reference	Acceptance Value	Content Uniformity(n=10) (RSD %)	Mean DHI Value computed on CLS distribution maps (n=10) ± Standard Error	Mean DHI Value computed on PCA distribution maps (n=10) ± Standard Error
A	1.10	0.46	2.066 ± 0.110	2.080 ± 0.114
B	4.54	1.60	2.333 ± 0.077	2.345 ± 0.071
C	8.64	3.56	2.445 ± 0.103	2.434 ± 0.104
D	23.31	8.29	3.051 ± 0.151	3.080 ± 0.154
E	29.41	11.04	3.491 ± 0.194	3.470 ± 0.196

Similarly, the calculated European Pharmacopoeia's acceptance values were plotted against the measured DHI values (Figure 5). Once again, a clear linear relationship is observed. It could therefore be possible to predict whether a formulation will have an acceptance value below the threshold of 15 or not with a defined uncertainty.

Based on DHI analysis of the distribution maps of the different formulations, formulation A was selected as the best formulation. Indeed, choosing this formulation ensures us that the formulation has the lowest content uniformity value and that its acceptance value is below the threshold value of 15.

Coefficients of determination with real samples are lower than those obtained with simulated images. This can be explained by sampling errors with real samples. Indeed, Raman hyperspectral imaging only analyzes the surface of the sample whereas content uniformity

values obtained by HPLC analyzes the whole tablet. Furthermore, only ten tablets per batch were tested (as recommended by the European Pharmacopoeia) but it is not really representative of a batch of about 100 000 tablets. Another parameter that must be optimized is the laser spot size and the spatial resolution of the hyperspectral analysis which are dependent on the particle size of the different present components.

All these sampling issues are under investigation to develop a generic approach that could be set up for any kind of homogeneity determination.

a. b.

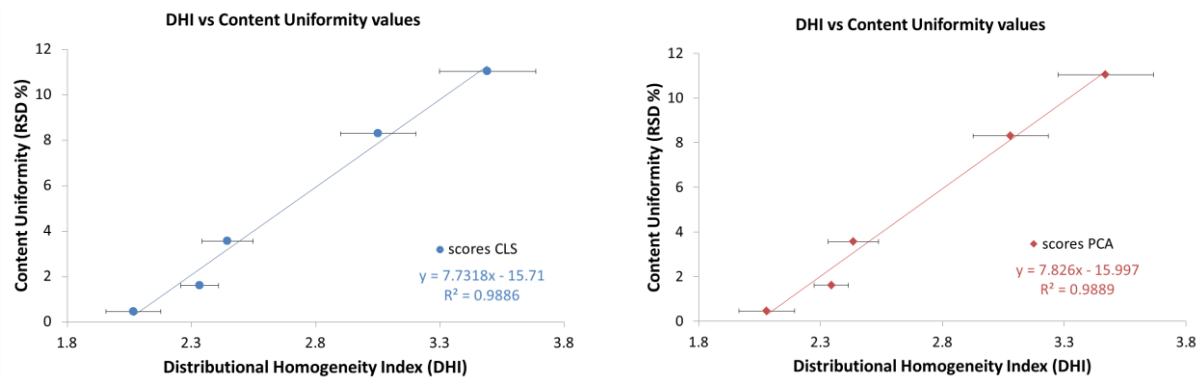

Figure 4: *a) Plot showing the relationship between the content uniformity values (RSD %) and the computed DHI values. DHI were computed with the distribution maps obtained by CLS analysis of the hyperspectral images of the tablet samples (see section 2). Each point represents the mean DHI value of ten tablets assorted with the corresponding standard error.*

b) Plot showing the relationship between the content uniformity values (RSD %) and the computed DHI values. DHI were computed with the distribution maps obtained by PCA analysis of the hyperspectral images of the tablet samples (see section 2). Each point represents the mean DHI value of ten tablets assorted with the corresponding standard error.

a. b.

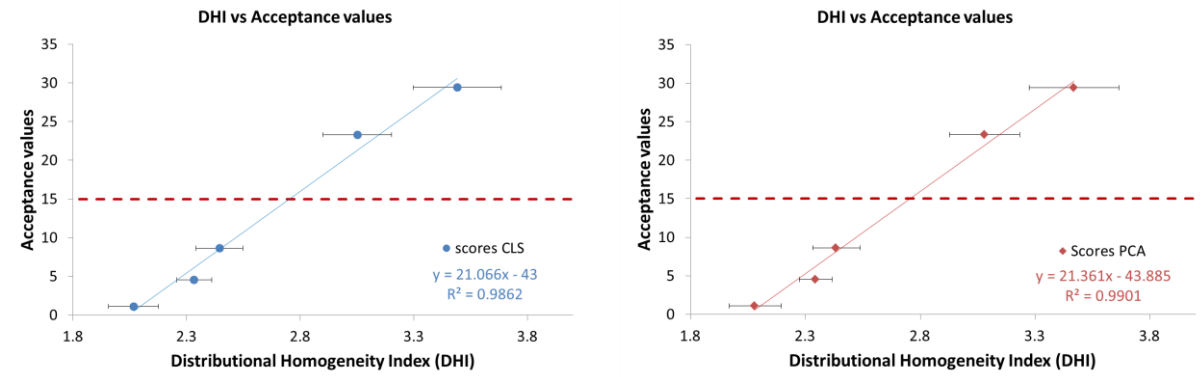

Figure 5: a) Plot showing the relationship between the European Pharmacopoeia's acceptance values and the computed DHI values. DHI were computed with the distribution maps obtained by CLS analysis of the hyperspectral images of the tablet samples (see section 2). Each point represents the mean DHI value of ten tablets assorted with the corresponding standard error. Red dotted line represents the maximal authorized acceptance value of 15.

b) Plot showing the relationship between the European Pharmacopoeia's acceptance values and the computed DHI values. DHI were computed with the distribution maps obtained by PCA analysis of the hyperspectral images of the tablet samples (see section 2). Each point represents the mean DHI value of ten tablets assorted with the corresponding standard error. Red dotted line represents the maximal authorized acceptance value of 15.

Conclusion

A new methodology for the assessment of spatial homogeneity in hyperspectral images has been presented. This methodology called Distributional Homogeneity Index (DHI) is based on the ratio of the area under the curve of the homogeneity curve of the raw studied map and the area under the curve of the homogeneity curve of the randomized studied map.

The DHI have been tested on simulated maps of increasing controlled homogeneity mimicking distribution maps of the studied compound. A linear relationship has been found between DHI values and controlled homogeneity. It has also been demonstrated that DHI values were dependent of map size. Therefore, to be compared, two tablets must be analyzed with the same parameters.

Simulated maps of the same size but with different proportions of zeros were tested. DHI values were, as presumed, dependent of the proportion of zeros. Therefore, two blend mixtures with very different proportions of the studied compound must be compared cautiously.

Nevertheless, it has been shown that DHI is a useful methodology to compare the distribution homogeneity of different blend mixtures during formulation development. This comparison is possible with distribution maps obtained without any calibration by CLS or PCA which lightens substantially the analysis work and enables a fast and non-destructive analysis of the samples.

The DHI approach has been tested on real samples of different pilot batches during formulation development. Linear relationship has been observed between DHI values and content uniformity values and with European Pharmacopoeia's acceptance values of the different batches allowing the selection of the most homogeneous formulation.

As with any application of hyperspectral imaging, sampling aspects are very important. This is why laser spot size, the spatial resolution and the achievement of a representative sampling of the studied batches are currently under investigation. The final objective is the elucidation of parameters to be optimized for the development of a generic approach of homogeneity assessment with hyperspectral imaging.

Acknowledgments

A research grant from the Belgium National Fund for Scientific Research (FNRS) to one of us (C. De Bleye) is gratefully acknowledged. Financial supports from the Walloon Region of Belgium are also gratefully acknowledged for the funding of E. Rozet, P.-Y. Sacré and L. Netchacovitch with the convention funds of N° 1217614, N° 1117469 and N° 1217716 respectively.

References

[1] T.R.M. De Beer, C. Bodson, B. Dejaegher, B. Walczak, P. Vercruysse, A. Burggraeve, A. Lemos, L. Delattre, Y. Vander Heyden, J.P. Remon, C. Vervaet, W.R.G. Baeyens, Raman spectroscopy as a process analytical technology (PAT) tool for the in-line monitoring and understanding of a powder blending process, J. Pharm. Biomed. Anal. 48 (2008) 772-779.

[2] A.S. El-Hagrasy, J.K. Drennen III, A Process Analytical Technology approach to near-infrared process control of pharmaceutical powder blending. Part III: Quantitative near-infrared calibration for prediction of blend homogeneity and characterization of powder mixing kinetics, J. Pharm. Sci. 95 (2006) 422-434

[3] T.R.M. De Beer, W.R. G. Baeyens, J. Ouyang, C. Vervaet, J.P. Remon, Raman spectroscopy as a process analytical technology tool for the understanding and the quantitative in-line monitoring of the homogenization process of a pharmaceutical suspension, Analyst 131 (2006) 1137-1144

[4] C. Gendrin, Y. Roggo, C. Collet, Pharmaceutical applications of vibrational chemical imaging and chemometrics : A review, J. Pharm. Biomed. Anal. 48 (2008) 533-553.

[5] J. Amigo, C. Ravn, Direct quantification and distribution assessment of major and minor components in pharmaceutical tablets by NIR-chemical imaging, Eur. J. Pharm. Sci. 37 (2009) 76-82.

[6] S. Piqueras, J. Burger, R. Tauler, A. de Juan, Relevant aspects of quantification and sample heterogeneity in hyperspectral image resolution, Chemometr. Intell. Lab. Syst. 117 (2012) 169-182.

[7] G.L. Alexandrino, R.J. Poppi, NIR imaging spectroscopy for quantification of constituents in polymers thin films loaded with paracetamol, Anal. Chim. Acta 765 (2013) 37-44.

[8] K.L.A. Chan, S.G. Kazarian, D. Vassou, V. Gionis, G.D. Chryssikos, In situ high-throughput study of drug polymorphism under controlled temperature and humidity using FT-IR spectroscopic imaging, Vib. Spectrosc. 43 (2007) 221-226.

[9] W.F.C. Rocha, G.P. Sabin, P.H. Março, R.J. Poppi, Quantitative analysis of piroxicam polymorphs pharmaceutical mixtures by hyperspectral imaging and chemometrics, Chemometr. Intell. Lab. Syst. 106 (2011) 198-204.

[10] W.H. Doub, W.P. Adams, J.A. Spencer, L.F. Buhse, M.P. Nelson, P.J. Treado, Raman Chemical Imaging for Ingredient-specific Particle Size Characterization of Aqueous Suspension Nasal Spray Formulations: A Progress Report, Pharm Res 24 (2007) 934-945.

[11] P-Y. Sacré, E. Deconinck, L. Saerens, T. De Beer, P. Courselle, R. Vancauwenberghe, P. Chiap, J. Crommen, J.O. De Beer, Detection of counterfeit Viagra by Raman microspectroscopy imaging and multivariate analysis, J. Pharm. Biomed. Anal. 56 (2011) 454-461.

[12] B. Vajna, A. Farkas, H. Pataki, Z. Zsigmond, T. Igricz, G. Marosi, Testing the performance of pure spectrum resolution from Raman hyperspectral images of differently manufactured pharmaceutical tablets, Anal. Chim. Acta 712 (2012) 45-55.

[13] N. Furuyama, S. Hasegawa, T. Hamaura, S. Yada, H. Nakagami, E. Yonemochi, K. Terada, Evaluation of solid dispersions on a molecular level by the Raman mapping technique, Int. J. Pharm., 361 (2008) 12–18.

[14] R.C. Lyon, D.S. Lester, E.N. Lewis, E. Lee, L.X. Yu, E.H. Jefferson, A.S. Hussain, Near-infrared spectral imaging for quality assurance of pharmaceutical products: Analysis of tablets to assess powder blend homogeneity, AAPS PharmSciTech 3 (2002) 1-17.

[15] C. Gendrin, Y. Roggo, C. Spiegel, C. Collet, Monitoring galenical process development by near infrared chemical imaging: One case study, Eur. J. Pharm. Biopharm. 68 (2008) 828-837.

[16] T. Furukawa, H. Sato, H. Shinzawa, I. Noda, S. Ochiai, Evaluation of Homogeneity of Binary Blends of Poly(3-hydroxybutyrate) and Poly(L-lactic acid) Studied by Near Infrared Chemical Imaging (NIRCI), Anal. Sci. 23 (2007) 871-876.

[17] T. Puchert, D. Lochmann, J.C. Menezes, G. Reich, A multivariate approach for the statistical evaluation of near-infrared chemical images using Symmetry Parameter Image Analysis (SPIA), Eur. J. Pharm. Biopharm. 78 (2011) 117-124.

[18] J.G. Rosas, M. Blanco, A criterion for assessing homogeneity distribution in hyperspectral images. Part 1: Homogeneity index bases and blending processes, J. Pharm. Biomed. Anal., 70 (2012) 680-690.

[19] J.G. Rosas, M. Blanco, A criterion for assessing homogeneity distribution in hyperspectral images. Part 2: Application of homogeneity indices to solid pharmaceutical dosage forms, J. Pharm. Biomed. Anal., 70 (2012) 691-699.

[20] J.G. Rosas, S. Armenta, J. Cruz, M. Blanco, A new approach to determine the homogeneity in hyperspectral imaging considering the particle size, Anal. Chim. Acta 787 (2013) 173-180.

[21] European Pharmacopoeia, 7th edition, European Directorate for the Quality of Medicines and Healthcare (EDQM), 2012, 4389-4391.

[22] P.H.C. Eilers, Parametric Time Warping, Anal. Chem. 76 (2003) 404-411.

[23] G.P. Sabin, A.M. de Souza, M.C. Breitkreitz, R.J. Poppi, Desenvolvimento de um algoritmo para identificação e correção de spikes em espectroscopia Raman de imagem, Quim. Nova 35 (2012) 612-615.

[24] J.A. Amigo, C. Ravn, Direct quantification and distribution assessment of major and minor components in pharmaceutical tablets by NIR-chemical imaging, Eur. J. Pharm. Sci. 37 (2009) 76-82.

[25] R. Tauler, Multivariate curve resolution applied to second order data, Chemometr. Intell. Lab. Syst. 30 (1995) 133-146.

[26] A. de Juan, R. Tauler, Chemometrics applied to unravel multicomponent processes and mixtures: Revisiting latest trends in multivariate resolution, Anal. Chim. Acta 500 (2003) 195-210.

[27] J. Jaumot, R. Gargallo, A. de Juan, R. Tauler, A graphical user-friendly interface for MCR-ALS: a new tool for multivariate curve resolution in MATLAB, Chemometr. Intell. Lab. Syst. 76 (2005) 101-110.

[28] W. Windig, J. Guilment, Interactive self-modeling mixture analysis, Anal. Chem. 63 (1991) 1425-1432.

[29] D.L. Massart, B.G.M. Vandeginste, L.M.C. Buydens, S. De Jong, P.J. Lewi, J. Smeyers-verbeke Handbook of Chemometrics and Qualimetrics-Part A, Elsevier Science, Amsterdam, 1997.

[30] M.L. Hamad, C.D. Ellison, M.A. Khan, R.C. Lyon, Drug product characterization by macropixel analysis of chemical images, J. Pharm. Sci. 96 (2007) 3390-3401.

[31] C. Ravn, Near-infrared Chemical Imaging in Formulation Development of Solid Dosage Forms Department of Pharmaceutics and Analytical Chemistry, Faculty of Pharmaceutical Sciences, University of Copenhagen, Denmark (2009) (Industrial PhD thesis).